Advances in Charged Particle Identification Techniques

Eugenio Nappi

INFN, Sezione di Bari, Bari, Italy

Abstract

The steady progress made over the past years in the design of innovative particle identification detectors has allowed to achieve relevant physics results in various experiments. The current investigation of new challenging approaches will seed future applications to the planned experiments at the SuperB factories and at the forthcoming FAIR facility, which demand an unrivalled particle identification performance. This paper will provide the current state of the art in the major charged particle identification techniques and will discuss the most significant advances and the most promising future directions.

Key words: Particle identification, TOF, dE/dx, ionization energy loss, RICH, DIRC, photocathodes, separation power, quantum efficiency

1. Introduction

In the process of studying the physics underlying the measurement, the capability to identify particles very often plays a prominent role in the determination of quark flavours in decays and in the enhancement of the signal from the background. It is well known that the development of innovative particle identification detectors (PID) has provided the very demanding hadron identification performance required to study CP violation in B meson decays and a successful operation in the very harsh environment produced by colliding gold nuclei head-on at RHIC. Technological advances have made the PID a robust experimental toolkit for the ALICE and LHCb experiments at the unprecedented energies of the LHC collider, whereas the design of the challenging PID systems of a new generation of experiments at FAIR and at the Super-B factories will depend critically on the ongoing R&D projects.

The choice of the PID technique is primarily dictated by the momentum range of the particles under study and by the required separation power[1], although other considerations (i.e. event rates, material budget, size and space requirements, accessibility, compatibility with other detector subsystems, coverage...) might be relevant as well.

A particle is univocally identified by its mass and electrical charge. The mass is obtained by measuring at least two out of the three correlated quantities: momentum, kinetic energy and velocity by exploiting the basic relationship $m = p/(c\beta\gamma)$ where β is the particle's velocity normalized to that of light in vacuum, c, and γ is the Lorentz factor $\gamma = E/mc^2$. Practically, the choice is restricted to the momentum and velocity: the particle tracking in a suitable static magnetic field provides the charge sign and the momentum value, whilst the velocity is obtained by means of one of the following methods: energy loss, time of flight (TOF), detection of Cherenkov radiation and, essentially for electrons, detection of transition radiation. Fig. 1 very schematically shows the momentum range in which a π-K separation of 3σ is achieved by the three major PID techniques, employing detectors of various lengths and performance. The same figure shows that, by varying opportunely the radiator medium, Cherenkov detectors covers the widest momentum range and allow to identify high momentum particles with reasonable detector sizes.

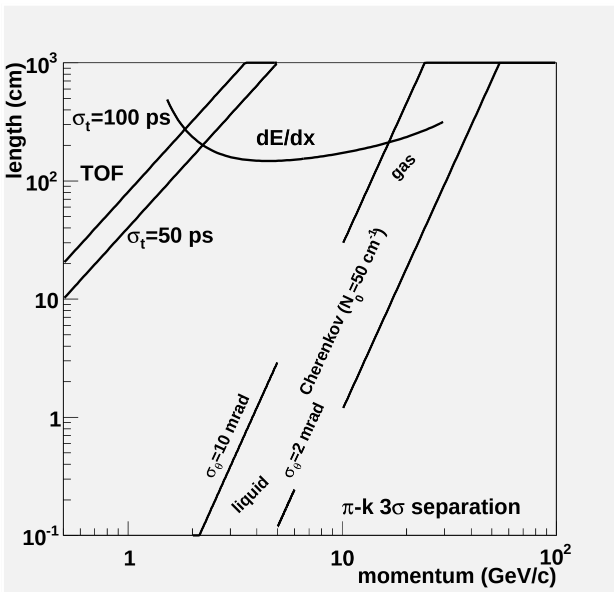

Figure 1: Momentum limit up to which a PID detector of a given length and performance achieves a 3σ π-K separation. For momenta above few GeV/c, only Cherenkov counters are able to feature such a separation power.

[1] The "separation power" of a PID system defines the significance of the detector response, S. If S_A and S_B are the mean values of such a quantity measured for particles of type A and B, respectively, and σ_{AB} is the average of the standard deviations of the measured distributions, the separation power n_σ is given by: $n_\sigma = \frac{S_A - S_B}{\sigma_{AB}}$.

The content of this paper is focused on the following methods: Time-Of-Flight (TOF), ionization energy loss measurements and Cherenkov light imaging and their applications to HEP experiments.

2. Time Of Flight

The identification of charged particles with a momentum larger than 1 GeV/c, through the measurement of their time of flight, requires a very good time resolution and a long flight path. The separation power $n_{\sigma_{t_{12}}}$ between two particles with masses m_1 and m_2, both of momentum p, over a flight path L, is given by: $n_{\sigma_{t_{12}}} = \frac{\Delta t_{12}}{\sigma_t} = \frac{L}{c\sigma_t}(\frac{1}{\beta_1} - \frac{1}{\beta_2}) \approx \frac{Lc}{2p^2\sigma_t}(m_1^2 - m_2^2)$ where σ_t is the time resolution of the TOF detector and $n_{\sigma_{t_{12}}}$ is the time difference between the two particles. The above equation entails that the length of the flight distance needed for particle separation at a fixed time resolution increases quadratically with the particle momentum. Therefore, the TOF technique is practical only for momenta below few GeV/c. As an example, a TOF system providing a time accuracy of 100 ps and 3.5 m of flight path discriminates $\pi - K$ with a separation power of 3σ up to a momentum of 2.1 GeV/c.

The determination of the particle velocity by means of time-of-flight measurements is carried out by exploiting either the light produced in scintillation counters or the formation and amplification of the ionization charge in very thin gaseous detectors. The technique based on scintillation counters is simple, well understood and robust. Particles traversing a scintillator bar excite molecules in the medium, the subsequent de-excitation results in the emission of a fluorescence light. These photons are collected by photomultipliers installed at both ends of each bar thus providing two independent measurements of the stop time and a $\sqrt{2}$ improvement in resolution. However, this technique is quite expensive and cannot be employed for TOF systems embedded in a magnetic field, unless fine-mesh PMTs are used instead of the cheaper standard PMTs. The best resolution that can be attained with "conventional" scintillation counters in a collider environment is optimistically around σ =100 ps. A more typical resolution, as overall obtained in experiments, is between 100 and 200 ps[1].

As mentioned earlier, a technological approach to fast timing based on thin gap gas counters has eventually attained a substantially good performance. The first example of a fast gas detector for TOF application was the Pestov counter, a 2 mm single-gap gaseous parallel plate chamber operated in spark mode[2]. It employed a semi-conductive ($10^9 \div 10^{10}\Omega$cm) glass as anode electrode and a special gas mixture at 12 bar. Although prototypes reached high efficiency (97%) and time resolution (40 ps), it was never employed in real experiments owing to a series of technological issues: extreme cleanliness and demanding production of large quantities of specific material (high resistivity glasses), high precision engineering (flatness better than a few μm), fabrication coating technology and accurate surface control procedures. Moreover, the operating gas contained 5000 ppm of 1.3 butadiene known as a potent cancerogene (max 1 ppm allowed in air).

A less ambitious R&D programme on PPAC (Parallel Plate Avalanche Chambers) and DRPC (Dielectric Resistive Plate Chamber), which resulted in time resolutions below 90 ps[3], proved the feasibility to build large area TOF systems with many channels as cost effective solution when compared to scintillator-based counters.

The real breakthrough was achieved by the ALICE Collaboration, which started a decade ago a systematic survey of the properties of the Multi gap Resistive Plate Chambers (MRPCs) for the construction of a 150 m^2 TOF barrel array. In this context, the crucial innovation was a detector made by many narrow gaps (few hundreds μm thin) operated at high gas gain yielding signals with a negligible time jitter[4].

The ALICE MRPCs consist of a stack of 400 μm thick 'off-the-shelf' soda lime glasses with a measured bulk resistivity of 2.4 10^{12} Ωcm and gas gaps of 250 μm (Fig.2).

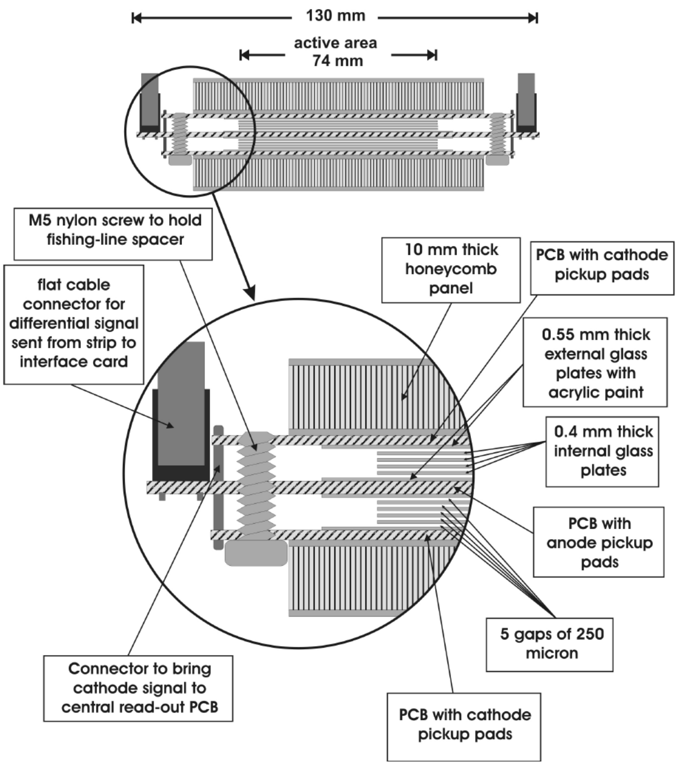

Figure 2: Cross section of the ALICE double-stack MRPC.

Electrodes are applied to the outer plates in order to feed HV via 10 MΩ resistors. The detector is filled with a non-flammable gas mixture containing $C_2H_2F_4$ (90%) + SF_6 (5%) + isoC_4H_{10} (5%). A detection efficiency higher than 99% and a mean time resolution lower than 50 ps have been achieved (Fig.3)[5].

As a result of tests at the Gamma Irradiation Facility (GIF) at CERN, MRPCs have shown a rate capability of up to 600 Hz/cm^2 for a continuous flux of charged particles. This good performance has been attained due to the small charge produced by each 'through-going' charged particle (on average 300 fC) and the low resistivity of the soda lime glass plates. An overall mean time resolution of about 90 ps has been measured by the

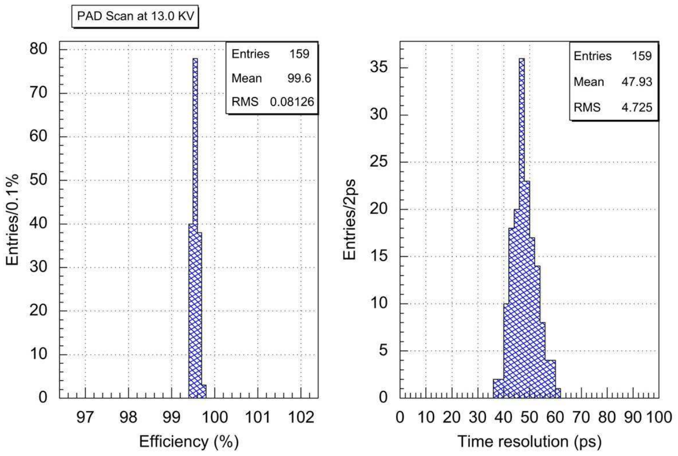

Figure 3: Efficiency (left) and time resolution (right) distributions for 159 read-out pads of an ALICE MRPC.

ALICE Collaboration during the cosmic ray test held in 2009 (Fig.4). The ALICE MRPC approach has also been adopted by the STAR experiment at RHIC for realizing a TOF barrel of 64 m^2[6] and it is under evaluation for the future CBM experiment at FAIR[7], which will be confronted with the selection of rare probes in a high multiplicity environment at collision rates of up to 10^7 events/sec. The design of the 100 m^2 CBM TOF will take advantage of the ongoing R&D activities for optimizing the MRPC glass resistivity in order to enhance the rate capability of these detectors up to several hundred kHz/cm^2[8].

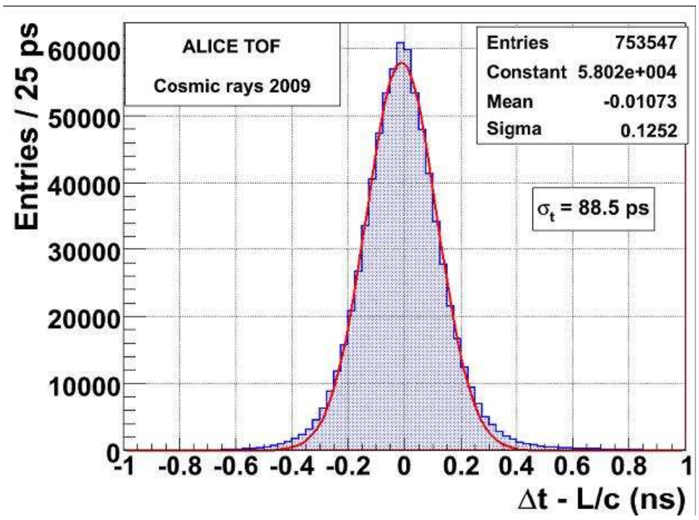

Figure 4: Time resolution distribution as measured by the full ALICE TOF barrel with cosmic rays.

2.1. Prospect

With the progress made in the development of fast photon detectors, like the Avalanche Photodiodes operated in Geiger mode (G-APDs) and the Microchannel plate photomultipliers (MCPs), the proposal [9] to build Cherenkov light based TOF counters becomes more and more feasible. These devices, equipped with thin quartz radiators, allow exploiting the excellent time and directionality properties of Cherenkov light rather than the scintillation light affected by the decay time of the scintillators and the jitter produced by the wide spread of photon paths from the emission point to the photon detectors. The potential pay-off is impressive: with the attained time resolution of $\sigma = 6.2$ ps[10] a π/K separation of 3σ can be achieved up to about 5 GeV/c for a flight path of 2 m. Several TOF R&D projects[11] have been triggered by the impressive properties of G-APDs and MCPs which, besides their excellent time resolution, are resistant to magnetic fields and feature a large photon counting capability.

3. Ionization energy loss

Ionization represents the main contribution to the energy loss in matter for charged particles and the primary mechanism underlying any detector technology. The velocity dependence of energy loss, $dE/dx \propto \ln(\beta^2\gamma^2)/\beta^2$, along with the momentum measurement, makes possible the determination of the particle mass.

The energy loss is large and scales like $1/\beta^2$ in the low momentum region, making very effective the particle identification there. The minimum in energy loss occurs at $\beta\gamma \sim 4$; in this momentum region, called cross-over or m.i.p. region, the method fails in discriminating particle species. The energy loss then rises slowly in the ”relativistic rise” region where modest separation may be possible. At higher momentum, the energy loss reaches the Fermi plateau due to the density effect.

The measurement of the ionization energy loss is carried out by means of gaseous or solid state counters, which provide signals with a pulse height proportional to the primary ionization produced in the sensitive volume. Although this is not an easy method for particle ID, it comes almost by free with the tracking devices and reduces confusion in associating the energy loss measurements with reconstructed tracks. However, the presence of the cross-over regions, where two particles of different mass but the same momentum produce an equal energy loss, and the saturation effect limit the range of application of this method. Moreover, since solid media are characterized by a small relative height of the Fermi plateau with respect to the minimum energy loss, particle identification in the relativistic rise region can only be performed with gas counters.

In the ionization measurements care must be taken to use a sensible estimator. In fact, not the *energy loss* by the particle is measured, but the *energy deposit* (sampled on each pad row), which is not necessarily the average energy lost in the given slice of material. As a result, the measurement is affected by large fluctuations in the number of created electrons per unit length, which are not poissonian-distributed. In fact, although the ionization energy loss is statistically distributed around its mean value, the formation of δ-electrons, having energies comparable with the energy loss of a particle in the counter, gives rise to an asymmetry in the distribution in energy loss, which shows a tail towards high energies. The resulting distribution, called Landau, after L. Landau, the Russian theorist who first calculated this process, is more asymmetric in a thin medium layer because of the large fluctuations in the various processes of energy transfer due to the few collisions expected. As a consequence of these rare events, where a large energy loss occurs, the mean energy loss in a sample is significantly higher than the most probable energy loss. In absorbers whose thickness is such to absorb almost half of the particle's initial kinetic energy, the mean energy loss approaches the most probable value with the probability distribution function being approximately Gaussian. However, because of the "Landau tail", the statistical precision in determining the mean of the distribution does not increase in the same way as for the Gaussian distribution if the thickness of the material traversed, and consequently the number of charges produced, increases. Due to the above drawbacks, a simple mean value would be a bad estimator. The practical way to improve the resolution is to measure the energy loss either in many consecutive thin detectors, thus minimizing the probability of generating a δ-electron of dangerously long range, or in a large number of samples, in the same detector volume, along the particle track. Subsequently, the mean of the lowest 60%-80% of measured ionization values is taken. An alternative method, which takes into account the full information on the charge development process, is based on the Bichsel functions[12]. The resulting parametrization is eventually fitted to the data or compared to the expectation. Both methods reduce the fluctuations in the calculation of the mean and permit a measurement of energy loss precise enough to achieve resolutions in the range 3÷10% for gaseous trackers (Table1). From Table1, the following conclusions can be drawn:

- Better resolutions are obtained with pressurized and/or large scale detectors (i.e. long effective track length). As the pressure is increased, the relativistic rise saturates at lower $\beta\gamma$; the optimal pressure seems to be about 4÷5 bar;
- In helium based detectors (BaBar, BELLE, CLEO III), the low ionization statistics is compensated by fewer cluster fluctuations;
- A higher content of hydro-carbons gives better resolution (BELLE and CLEO III). In fact, the FWHM of Landau distributions is as large as 60% for noble gases, it decreases to 45% for CH_4 and it is only 33% for C_3H_8.

An accurate understanding of the detector parameters that influence the energy loss measurements is necessary to optimize the detector design. Very refined simulations, based on measured cross-sections of photon scattering on the most common types of atoms in the tracker's gas mixtures[13], allowed to find the following approximate empirical scaling relationship for the resolution on dE/dx:

$\sigma(dE/dx) \sim n^{-0.43\div-0.47}(t \cdot p)^{-0.32\div-0.36}$

It is worthwhile to notice that σ does not follow the $n^{-0.5}$ gaussian dependence owing to the Landau fluctuations and, fixed the total lever arm (nt), it is more effective to increase n rather than t, provided that the number of electron-ion pairs is enough in each sampling layer. On the basis of the previous equation, dE/dx measurements can be attained also for small devices, only 1 m long, with 60÷100 samples operating at 1 atm. With such devices, one can perform hadron-electron identification into the few GeV/c range, and hadron-hadron identification in the non-relativistic region (below 1 GeV/c) by either using heavy gases or increasing the gas pressure, in order to improve the resolution. In the relativistic region, this approach is not as effective because both the gas pressure and density can affect the size of the relativistic plateau. In fact, denser gases have a smaller relativistic plateau and by increasing the pressure one reduces the relative height of the relativistic plateau with respect to the minimum energy loss, thus destroying much of the advantage gained from smaller resolution. The pressure dependence of the relativistic rise can be parameterized approximately as follows:

relativistic rise $(Emax/Emin) \sim 1.6x(pressure)^{-0.09}$.

To achieve good hadron-hadron identification in the relativistic rise region, one must employ very large devices (longer than 150 cm) operated at high gas pressure, with many samples. Gas composition plays a minor role for the achievable performance.

3.1. Time Projection Chambers

The ultimate detector for performing an outstanding combined tracking and ionization energy loss measurement is the Time Projection Chamber (TPC). In a collider experiment, the TPC's field cage is divided into two halves by a planar central electrode represented by a thin membrane and by two endcap multi wire proportional chambers (MWPCs). The primary electrons produced by ionizing particles slowly drift toward the MWPC's amplifying region where a gating grid allows their passage when triggered. If the gate is opened, avalanches are created and recorded as charge induced signal on cathode pads. The charge recorded on adjacent pads enables an accurate determination of the position by means of the evaluation of the center of gravity. The third coordinate of the primary ionization is achieved by measuring the time taken by the trail of ionization electrons to drift to the plane of wires and pads. These features make TPCs the best tracking devices to be used in high multiplicity experiments (heavy ion collisions at RHIC and LHC) and for jet physics.

The STAR and ALICE TPCs are quite remarkable examples of large volume devices able to reconstruct and efficiently identify a thousand tracks per event (Fig. 5). The ALICE TPC, with a field cage 5 m long and a total sensitive volume of 88 m^3, is currently the largest gaseous tracker ever built in the world[14]. The need to achieve a good momentum resolution and to keep small the distortions created by the space charge has induced the ALICE Collaboration to adopt a drift gas with low diffusion, low Z and large ion mobility. Extensive investigation of various gas compositions led to the choice of the mixture: Ne(85.7%)-CO_2(9.5%)-N_2(4.8%). This drift gas, characterized by a non-saturated drift velocity (cold gas), requires a thermal stability of 0.1 K and a high drift field (400 V/cm) to secure an acceptable drift time of 88 μs. Therefore, the high voltage on the central electrode has to be as high as 100 kV. An insulating envelope filled of CO_2 gas surrounds the actual field cage for operational safety reasons and acts as a thermal screen.

The readout chambers are conventional MWPCs with cathode planes segmented in pads equipped with an electronics

Table 1: Summary of selected design parameters of significative examples of gas based dE/dx systems (n = number of samplings, t = thickness of the sampling layer, p = gas operational pressure). Also listed is σ = resolution of the mean ionization energy loss.

Experiment	Detector type	n	t(cm)	p(bar)	Gas composition	σ(%)
BELLE	Drift chamber	52	1.5	1	He/C_2H_6=50/50	5.5
BaBar	Drift chamber	40	1.2	1	He/i-$C_4H_1$0=80/20	7.5
CLEO III	Drift chamber	47	1.4	1	He/C_3H_8=60/40	5.0
ALEPH	TPC	338	0.4	1	Ar/CH_4=90/10	4.5
PEP	TPC	183	0.4	8.5	Ar/CH_4=80/20	3.0
OPAL	Jet chamber	159	1.0	4	Ar/CH_4/i-$C_4H_1$0=88.2/9.8/2	2.8
STAR	TPC	44	1.15-1.95	1	Ar/CH_4=90/10	7.5
ALICE	TPC	72	1.5	1	$Ne/CO_2/N_2$=85.7/9.5/4.8	5.5
T2K	TPC with MM	72	1.5	1	Ar/CF_4/i-$C_4H_1$0=95/3/2	10

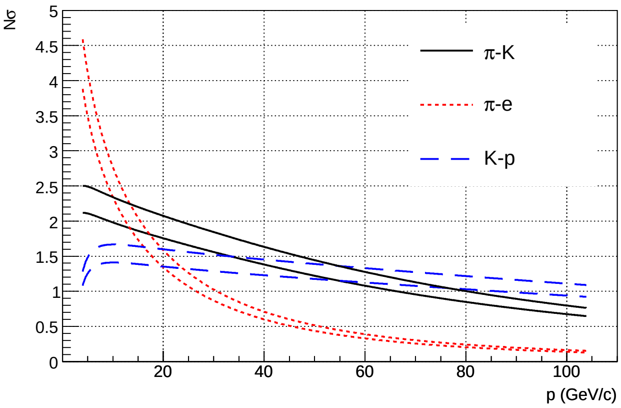

Figure 5: Projected separation power of the ALICE TPC as a function of the particle momentum. The performance has been estimated for two particle densities: $dN/d\eta$=800 (upper curves) and $dN/d\eta$=8000 (lower curves).

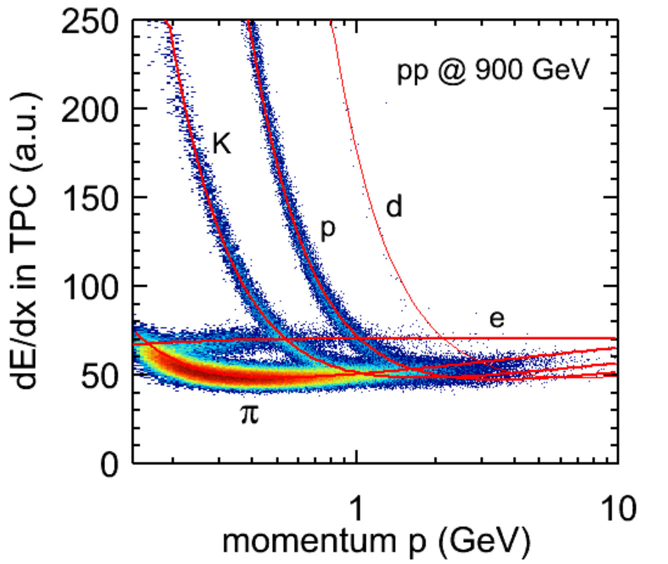

Figure 6: Ionization energy loss spectrum as obtained by the ALICE TPC with tracks from almost 10 million events of pp collisions at LHC.

chain to amplify, digitize and pre-process the signal before transmission to the DAQ. Each of the 570,000 channels includes a custom digital circuit that, with an innovative approach, performs tail cancellation, digital baseline restoration, data compression and multi-event buffering for event derandomization. The azimuthal segmentation of each readout plane consists of 18 trapezoidal sectors, each covering 20 degrees. The impressive results obtained with tracks belonging to ten millions of events collected in 2009 from LHC pp collisions (Fig. 6) show the correctness of the design and construction of the huge ALICE tracker.

The ALICE project was indeed very challenging especially if one takes into account that the incorporation of dE/dx measurement in a TPC requires that a number of tight engineering constraints be enforced, especially all mechanical tolerances, wire staggering, electrostatic and gravitational deflections must be carefully controlled and their stability ensured. Moreover, possible background problems, associated space charge effects and gating efficiency had to be accurately evaluated to avoid negative effects in the tracking and in the dE/dx sampling.

3.2. Prospect

An important innovation in the design of the future TPCs concerns the endplate readout detectors by the replacement of MWPCs with MPGDs (Micro-Pattern Gas Detectors), like GEMs (Gaseous Electron Multiplier) or a Micromegas (MICRO-Mesh GASeous detector). Among the MPGDs features, the following ones provide quite relevant advantages:

- negligible $\vec{E} \times \vec{B}$ effect (due to the bi-dimensional symmetry of the amplifying structures);
- intrinsic ion feedback suppression (leakage smaller than 1-2%);
- more flexibility in the readout structures.

In particular, the absence of the $\vec{E} \times \vec{B}$ effects makes TPCs equipped with MPGDs capable of operating at large magnetic fields (3-5 T). The resulting benefits are a reduced transverse diffusion and an improved spatial resolution.

The first application of MPGDs to a real experiment has occurred in the long baseline neutrino oscillation experiment

T2K [15] at JPARC (Japan). Bulk Micromegas, based on commercial woven meshes, have been used in the three T2K's TPCs for covering a total active area of about 9 m^2.

The poor particle separation power attainable by means of the ionization energy loss measurements could be improved by exploiting the cluster counting approach. In this respect, MPGDs associated to the silicon pixel technology[16] may play a prominent role by significantly improving the dE/dx resolution. In fact, this innovative technique could provide the high granularity needed to resolve individual clusters which are separated by average distances between them of about 300 μm (30 clusters/cm). Direct cluster counting of primary ionization would also be a benefit from the operational point of view because it is not affected by gas gain instabilities since no charge measurements are performed but just counting. Moreover, it would be an unprecedented potential for pattern (track) recognition and track fitting in dense track environments for the better double hit/track resolution attainable and the possibility to get rid of delta rays. This innovative technique has already proved the feasibility to detect individually single electrons from the ionizing particles, but more studies are needed to assess its capability to perform cluster counting.

4. Cherenkov Light Imaging

The measurement of the Cherenkov angle via the direct imaging of the emitted photons is nowadays the basis of a well-established technique, largely employed in high-energy and astro-particle physics experiments to achieve the identification of charged particles in an impressively vast momentum range from a few hundred MeV/c up to several hundred GeV/c[17]. This technique comprises two main categories: RICH (Ring Imaging CHerenkov) and DIRC (Detection of Internally Reflected Cherenkov) devices.

In a RICH detector, Cherenkov radiation emitted in a transparent dielectric medium, called the radiator, whose refractive index is appropriate for the range of particle momentum being specifically studied, is transmitted through an optics, which could be either focusing with a spherical (or parabolic) mirror or not focusing (proximity-focusing), onto a photon detector that converts photons into photoelectrons with high spatial and time resolutions (Fig. 7).

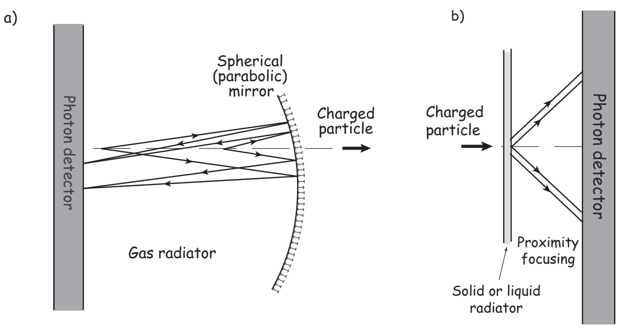

Figure 7: Working principle of a RICH detector: a) focusing scheme, b) proximity-focusing scheme.

The DIRC[2]concept is based on the exploitation of the fraction of light trapped by total internal reflection inside long bars of quartz. It basically uses a "pinhole" geometry, where the bar's exit area, together with a photon detecting pixel position, define the photon exit angles in 2D; the time and the track position defines the third coordinate (Fig. 8). Counters based on Cherenkov light imaging can handle high multiplicity events since photoelectron footprints from several particles in the same event are visualized onto the plane of detection thus allowing the determination of the emission angle θ_c for each detected photon. The mass m of a particle of known momentum p is eventually given by $m = p(n^2cos^2\theta_c - 1)^{1/2}$.

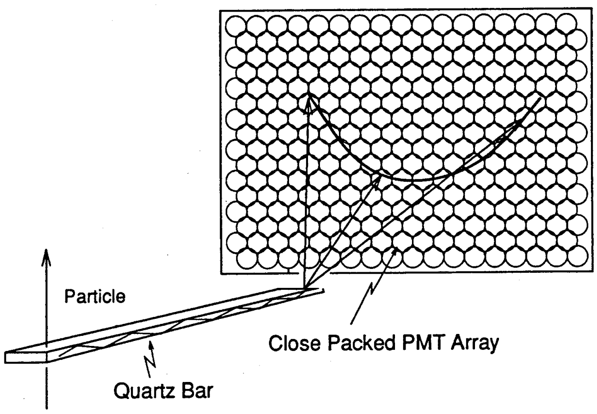

Figure 8: Working principle of a DIRC detector.

A Cherenkov light imaging detector with a figure of merit N_0 and a radiator characterized by the refractive index n and total length L measures the Cherenkov angles θ_1 and θ_2 of two particles of momentum p and masses m_1 and m_2 respectively, with an accuracy defined by the number of standard deviations $N\sigma_c$ such that $\theta_2 - \theta_1 = N\sigma_c$. It follows that the largest momentum limit is achievable by designing counters able to detect the maximum number of photons (large N_0) with the best angular resolution (small θ_c). The examples discussed below highlight a few of the recent achievements and will provide a general impression of what is to be expected in the two categories. Emphasis will be given to the development of efficient single photon detectors because of their paramount importance as basic ingredient for this technique.

4.1. RICH detectors

During the last years, the development of large area photocathodes made of thin films of CsI[18] has significantly contributed to extend the potentiality of the RICH technique. Large area MWPCs equipped with a CsI photocathode working in reflective mode with electron extraction in CH_4 at atmospheric pressure have successfully been implemented in the RICH counters of COMPASS[19], Hades[20] and at the JLAB-Hall A facility[21]. The largest application of this technique

[2]DIRC uses internally reflected Cherenkov light, which is opposite to the CRID detector at SLD, which used the transmitted Cherenkov light (therefore, the letters in the two names are backward).

(11 m^2 of photon sensitive surface) is, however, the CsI RICH of the ALICE[22] experiment, which has recently completed the commissioning phase and has started to take data at LHC. On the side of vacuum based photon detectors, the improvement in the performance of "off-the-shelf" multi-anode photomultipliers (MaPMTs) has allowed the COMPASS Collaboration to achieve the desired PID capability also in the very forward region of their set-up, severely affected by the beam halo[23].

A different approach has been followed to equip the focal planes of the two LHCb's RICH counters, designed to identify hadrons in the momentum range from 1 to 100 GeV/c. The demanding request of handling almost 0.5 million channels at the high acquisition rates expected at LHC pushed the LHCb Collaboration to develop, in collaboration with industry, large area hybrid photon detectors (HPDs)[24]. The LHCb RICH counters successfully started data taking in 2009.

The RICH systems of LHCb, COMPASS and the forthcoming NA62 experiment at CERN[25] are good examples on how improvements on both operation and performance are achieved by designing RICH detectors that operate in the visible light region. In fact, at longer wavelengths the detector figure of merit becomes larger as a consequence of the higher material transparency, which enlarges the bandwidth. Also the angular accuracy for the single photon improves due to the reduced chromatic aberrations of materials in the visible region.

The use of visible light photon detectors has also allowed the exploitation of silica aerogel as Cherenkov radiator in a momentum range not accessible to other materials[26]. Following the development of clear hydrophobic tiles for Belle, the combination of aerogel radiator with a gas radiator (C_4F_{10}) in the same RICH counter was pioneered by the HERMES experiment[27] and subsequently employed by LHCb. The recent production of silica aerogel tiles manufactured as a stack of two to four layers of slightly different refractive indices has driven the design of the proximity focusing aerogel RICH detector (Fig. 9) envisaged to identify particles in the forward direction (endcap) of SuperBelle[28].

The anticipated π/K separation power at 4 GeV/c is almost 6σ, further investigation is ongoing to select the type of photon detector to use. G-APDs, Hybrid Avalanche Photodiodes (HAPDs) or MaPMTs are possible candidates. Despite the considerable progress made in the field of vacuum based photon detectors and G-APDs, their high cost and low photon detection efficiency due to the small packing factor make these devices less attractive when the coverage of large photon collection areas is required. In this case, gaseous detectors represent the most effective solution and, in particular, GEM based photon detectors seem the most obvious choice for future experiments. In order to achieve a high single-photon detection efficiency, a multilayer structure GEM is used. The first layer, coated with a CsI film, acts as a reflective photocathode; gains above 10^5 are reached in the avalanche induced by the photo-electron.

The PHENIX experiment at RHIC has been the first to apply GEMs in realizing the Cherenkov threshold counter called Hadron Blind Detector (HBD)[29].

At very high rates, however, GEMs suffer photocathode ageing and detector electrical instability due to the photocathode bombardment by the ions generated during the charge multiplication process, which back-flow to the CsI film. In order to overcome such a limitation, the design of innovative ion blocking architectures has been proved to trap most of the ions reaching a fraction of those back-flowing as small as 10^{-4} at gains of 10^5 with full single-photoelectron collection efficiency[30]. This breakthrough will pave the road towards the design of a visible-sensitive gaseous photomultiplier working at high gains in DC mode. The main challenge of this development is given by the extreme chemical reactivity of bialkali.

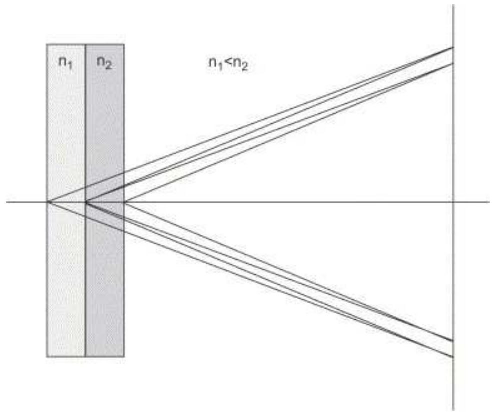

Figure 9: Scheme of the proximity focusing RICH detector with a multilayer aerogel radiator in the focusing configuration.

Recent advances in the deposition technique have shown that K_2CsSb, Cs_3Sb and Na_2KSb photocathodes are quite stable in a gas chamber[31]. A quantum efficiency above 30% in the range from 360 nm to 400 nm has been measured for K_2CsSb photocathodes in presence of Ar/CH_4(95/5) gas mixture. As a parallel development, the COMPASS and ALICE experiments are studying thick GEM (THGEM) for low interaction rate applications. In these counters, the Cu-coated kapton foils of the standard GEM counters is replaced by 0.4-1 mm thick PCB layers with holes of 0.3-1 mm diameters mechanically drilled. The large hole-size results in a good electron transport and in large avalanche-multiplication factors (up to 10^7 in double-THGEM cascaded single-photoelectron detectors). The easiness of THGEM's mechanics (standard printed-circuit drilling and etching technology) and implementation, which does not require any special mechanical supports, allows manufacture of large detector areas.

A second type of thick GEMs, called resistive THGEM (RETHGEM)[32], has also been designed to conceive a spark-immune photo-multiplier but at expense of lower counting-rate capability (in the range 10÷100 Hz/mm^2). RETHGEMs are made by silk-screen printing techniques, which allow production of large areas up to 50x50 cm^2 with the possibility to adjust the electrode resistivity to the experimental needs. Gains above 10^5 were reached in double RETHGEM coupled to a CsI photocathode[33].

4.2. DIRC-like detectors

DIRC counters will play a decisive role at FAIR (PANDA and CBM experiments) and in the second generation B-factories to cope with the high rates and to improve the separation capabilities for rare decay channels.

The design of the second generation DIRC envisages the use of finely segmented high speed photon detectors and a focusing optics instead of the current pin-hole geometry. The latter is meant to reduce the error due to the bar size whereas the use of fast visible light photon detectors (with a time resolution in the range of 50÷100 ps per single photon) will likely correct the chromatic error by timing. This remarkable approach, conceived by B. Ratcliff[34], has been demonstrated by BABAR teams[35], who succeeded to reduce by about 1 mrad the chromaticity smearing of the Cherenkov angle by measuring the energy of each detected Cherenkov photon via its arrival time at the detection device. Fast timing also helps in suppressing the strong background expected at the unprecedented high luminosities of the forthcoming facilities, as the future Super B-factories are planned to deliver a 100-fold increase in luminosity.

The PANDA Collaboration is also planning to use the DIRC concept for the hadron ID system of their experiment at the HESR of the future FAIR facility at GSI. Very interesting in this context is their idea to correct the radiator dispersion using passive optical elements made of LiF crystals[36].

The PID option considered at SuperBelle is the Time-of-propagation (TOP) counter in the barrel region which uses time of arrival to determine the Cherenkov angle[37]. TOP has the great advantage to reduce the costs of the photon detector. In fact the DIRC PMT wall will be replaced by a one-dimensional readout since one coordinate is obtained by the timing information of the detector.

The feasibility of the TOP counter has already been demonstrated in beam tests using 16 channel MaPMTs. The TOP detector is very challenging because the photon detectors have to feature a single photon time resolution smaller than 100 ps and have to be compatible with high magnetic fields (up to 1.5 T). The goal is to achieve a separation power of 4.2σ at 4 GeV/c, to be compared with the anticipated value of 3.5σ of the focusing-DIRC.

A cutting edge approach has been proposed by the Belle Collaboration through the development of a GaAsP photo-cathode MCP-PMT[38] characterized by a QE at longer wavelengths higher than that of an alkali photo-cathode. This device will likely allow achieving a better resolution in the measurement of the arrival time of propagated photons because of the radiator's smaller chromaticity towards the red wavelengths. The main drawbacks of adopting MCP-PMTs as Cherenkov photon detectors are their low photon detection efficiency, rate instability and reduced lifetime. These issues are faced by the current R&Ds in collaboration with industry.

5. Summary

The following significant advances in the PID techniques have recently emerged and will allow applications unexpected still a few years ago.

The particular benefit of using gaseous MRPC is among the major accomplishments of the past years in the TOF technique. The availability of very fast photon detectors achieving time resolutions of a few tens of ps will enrich very much the performance of the TOF technique in the coming years, thus allowing unprecedented PID capabilities.

The longstanding challenge provided by the cluster counting method needs to be soon addressed. It will be essential for the improvement of the PID technique by the measurement of the ionization energy loss. The combination of MPGDs with pixel technology may have the potential to shed light on this field.

The relevance of the chromatic error on the achievable separation power of Cherenkov light imaging detectors makes very fast photon detectors play a prominent role in the current R&D projects. Innovative designs employing chromatic correction through the measurement of the photon arrival times are being developed in view of the challenging PID required at FAIR and at the future SuperB factories.

6. Acknowledgements

It has been a privilege and a pleasure to have contributed to the success of VIC2010 with a review talk on advances in PID techniques. I am very grateful to the organizers and the ISAC members for the invitation.

References

[1] N.V.Rabin, Instruments and Experimental Techniques, 2007, Vol. 50, No. 5, pp. 579-638
[2] H.R. Schmidt, Nucl. Phys. B (Proc. Suppl.) 78 (1999), p. 372.
[3] A. Akindinov *et al.*, Nucl. Instr. and Meth. A 494 (2002) 474.
[4] ALICE-TDR of the TOF, CERN/LHCC 2000-12, ALICE TDR 8, 16 February 2000, and references therein.
[5] A. Akindinov *et al.*, Nucl. Instr. and Meth. A 602 (2009) 709.
[6] Y. Wang *et al.*, Nucl. Instr. and Meth. A 613 (2010) 200.
[7] Letter of Intent for the CBM Experiment, Darmstadt, Germany (2004).
[8] L. Naumann, "Ceramics high rate timing RPC", at VCI2010 conference (this volume).
[9] Y. Enari *et al.*, Nucl. Instr. and Meth. A 547 (2005) 490 and K. Inami *et al.*, Nucl. Instr. and Meth. A 560 (2006) 303.
[10] K. Inami, R&D of particle identification devices with high-precision timing, Nucl. Instr. and Meth. A in press.
[11] Workshop on Large-Area-Picosecond-Photodetectors electronics for Particle Physics and Medical Imaging, January 28th and 29th 2010, Clermont Ferrand (France) http://clrwww.in2p3.fr/www2008/WTDMPPA/
[12] H. Bichsel, Nucl. Instr. And Meth. A 562 (2006) 154.
[13] W.W.M. Allison and J. H. Cobb, Ann. Rev. Nucl. Sci. 30 (1980) 253.
[14] ALICE Technical Design Report of the Time Projection Chamber CERN/LHCC 2000-001, ALICE TDR 7 and ALICE Physics Performance Report Volume 1 CERN/LHCC 2003-049, ALICE PPR Volume 1.
[15] K. Kaneyuki *et al.*, Nucl. Phys. B - Proceedings Supplements Vol. 145, 2005, 178-181
[16] H. van der Graaf, Nucl. Instr. and Meth. A 604 (2009) 5.
[17] E. Nappi and J. Seguinot, Rivista del Nuovo Cimento, 28, 1-130.
[18] A. Hoedelmoesser *et al.*, Nucl. Instr. and Meth. A 553 (2005) 140.
[19] E. Albrecht *et al.*, Nucl. Instr. and Meth. A 553 (2005) 215.

[20] K. Zeitelhack *et al*. [HADES Collaboration], Nucl. Instr. and Meth. A 433 (1999) 201; L. Fabbietti *et al*. [HADES Collaboration], Nucl. Instr. and Meth. A 502 (2003) 256.
[21] M. Iodice *et al*., Nucl. Instr. and Meth. A 553 (2005) 231.
[22] A. Gallas *et al*., Nucl. Instr. and Meth. A 581 (2007) 402.
[23] P. Abbon *et al*., Eur. Phys. J. Special Topics 162, 251-257 (2008).
[24] S. Eisenhardt [LHCb RICH Collaboration], Nucl. Instr. and Meth. A 565 (2006) 234.
[25] M. Lenti, Nucl. Phys. B (Proc. Suppl.) 197 (2009) 117-120.
[26] E. Nappi, Nucl. Phys. B (Proc. Suppl.) 61 (1998) 270.
[27] R. De Leo, Nucl. Instr. and Meth. A 595 (2008) 19.
[28] T. Ijima *et al*., Nucl. Instr. and Meth. A 595 (2008) 92.
[29] B. Azmoun *et al*.IEEE Transactions 57:3 1544-1549 (2009).
[30] A. V. Lyashenko *et al*., Nucl. Instr. and Meth. A 598 (2009) 116.
[31] A.V. Lyashenko *et al*., JINST 4 (2009) P07005.
[32] A. G. Agcs, *et al*., Nucl. Instr. and Meth. A 595 (2008) 128.
[33] C.D.R. Azevedo *et al*., 2010 JINST 5 P01002.
[34] B.Ratcliff, Nucl. Instr. and Meth. A 502 (2003) 211.
[35] J.Benitez *et al*., Nucl. Instr. and Meth. A 595 (2008) 104.
[36] P. Schnmeier *et al*., Nucl. Instr. and Meth. A 595 (2008) 108.
[37] K. Inami, Nucl. Instr. and Meth. A 595 (2008) 96.
[38] T. Ijima, Nucl. Instr. and Meth. A 598 (2009) 138.